J. Amer. Soc. Hort. Sci. 127(2):303–308. 2002.

Application of Time-of-flight Near-infrared Spectroscopy for Detecting Water Core in Apples

Satoru Tsuchikawa,[1] Sanae Kumada, and Kinuyo Inoue
Graduate School of Bioagricultural Sciences, Nagoya University, Nagoya 464-8601, Japan

Rae-Kwang Cho
Department of Agricultural Chemistry, Kyungpook National University, Taegu 702-701, Korea

Additional index words. *Malus sylvestris* var. *domestica* 'Fuji', time resolved profile, pulsed laser beam

Abstract. **Time-of-flight near-infrared spectroscopy (TOF-NIRS) was used to investigate optical characteristics of water-cored tissue in 'Fuji' apples [*Malus sylvestris* (L.) Mill. var. *domestica* (Borkh. Mansf.)]. The combined effects on the time resolved profiles of water core, laser beam wavelength, and detection position of transmitted light were investigated in detail. Attenuance of peak maxima (A_t), time delay of peak maxima (Δt), and variation of full width at half maximum (Δw) decreased gradually as water core increased. Water-cored tissue transmitted much more energy because of the filling of intercellular spaces with liquid, so that the light path time through a sample decreased. These parameters were also strongly dependent on detection position and wavelength of the laser beam. The substantial optical path length calculated from Δt at λ = 800 nm was 10 to 17 times, while that for λ = 900 nm varied from six to 11 times the distance of the diameter of the fruit. Results indicated the optimum optical parameter for detection of water core was Δt.**

Consumer demands with respect to agricultural products are becoming increasingly diverse. The producer must not only supply them safely while maintaining freshness, but also needs to assure the taste and nutritional values. Therefore, a nondestructive measurement system that can accurately monitor these indices simultaneously with minimum time and effort is very desirable for marketing of agricultural commodities.

In the past few decades, many researchers have focused on the potential use of near infrared spectroscopy (NIRS), a practical spectroscopic procedure, for detection of organic compounds in matter. In the fields of food, medicine, paper, etc., intense interest has been directed towards NIRS because of its accuracy and rapid response (Burns and Ciurczak, 1992; Osborne, et al., 1993).

Detection of near infrared (NIR) light from a sample is by either transmittance or reflectance. The transmittance NIR method is very desirable for detecting internal information, whereas the optical information from diffuse reflectance spectra is confined to the subsurface layer of samples. It is especially important that progress be made in developing an NIR transmission device for detection of internal characteristics of high moisture fruit and vegetable products. With respect to this need, Kays (1999) presented an overview of application of NIRS to horticultural sciences. For example, nondestructive detection of water core in apples (*Malus sylvestris* var. *domestica*) would be of considerable value to the fresh apple industry. When sorbitol accumulates in the core area of an apple, a so-called water core is formed. In many countries, water-cored apples can be consumed at harvest time as high quality fruit, however, such apples can not be stored successfully as they are particularly perishable. Water-cored apples can not be distinguished externally from sound fruit, as the water core is formed literally in the core area of apple. Therefore, it is essential to utilize a transmitted light beam for its nondestructive detection.

A number of techniques and devices using transmittance or reflectance for examining apples (e.g., sugar content or water core) were proposed previously (Birth and Olsen, 1964; Cho et al., 1998; Hwang and Noh, 2000; Meurens and Moons, 2000). However, behavior of transmitted light from an agricultural product is directly affected by physical and chemical properties of the tissues, making it very important to examine in detail the optical characteristics of the tissue and the output origin of transmitted light in detail from a new viewpoint (i.e., estimating the substantial optical path length in the sample). Recently, the authors constructed optical characteristic models to provide a background and framework for developing a nondestructive measurement system applicable to biological materials having a woody cellular structure (Tsuchikawa and Tsutsumi, 1999a, 1999b; Tsuchikawa et al., 1996). These nontraditional applications of NIRS, based on diffuse reflectance spectra, made possible analysis of both physical conditions and chemical components of biological material while retaining its cellular structure, although the optical information was confined to the subsurface layer of samples. Furthermore, to determine wide application of NIRS to a thick sample, we established a high power measurement system which was comprised of a semiconductor NIR laser and the thermocouple power meter (Tsuchikawa et al., 2000b). In this case, the selection of a wavelength for such a device should be limited by its quantum mechanical characteristics.

Some researchers have reported previously on the properties of light scattering in various samples (Profio, 1989; Sevick et al., 1991). Leonardi and Burns (1999a, 1999b) investigated quantitative measurements in scattering media on the basis of time-of-flight (TOF) analysis with analytical descriptions. They reported that experimental analysis of the time resolved profile was very efficient for estimating the absorption and scattering coefficient. Their study was the first attempt to differentiate sound and water-cored apples by TOF near infrared spectroscopy (TOF-NIRS). On the basis of these results, we examined development of a new system, by which the constituent, water core (or defective portion of an apple) can be detected exactly. In this study, an optical measurement system comprised of a parametric tunable laser and a near infrared photoelectric multiplier, was introduced to accomplish this purpose from the viewpoint of TOF-NIRS. This system combined the best features of the spectrophotometer and the laser beam, and more advantageously, the time resolved profile of transmitted output power could be measured sensitively in nanoseconds. The combined effects on time resolved profiles of the

Received for publication 20 Mar. 2001. Accepted for publication 28 Nov. 2001.
[1]Corresponding author. E-mail: st3842@agr.nagoya-u.ac.jp.

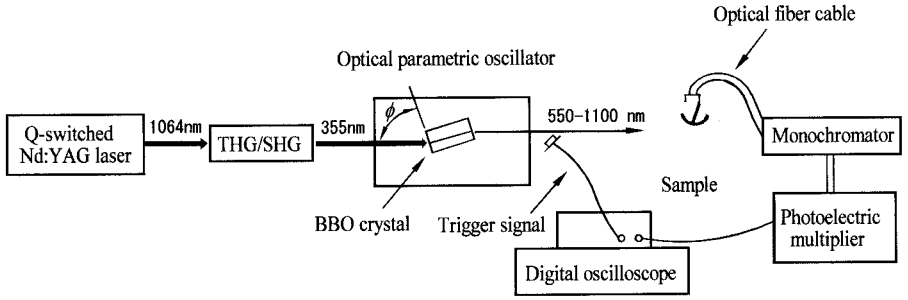

Fig. 1. Schematic diagram of measuring system used for the detection of water core in apple. THG = third harmonic generator and SHG = second harmonic generator.

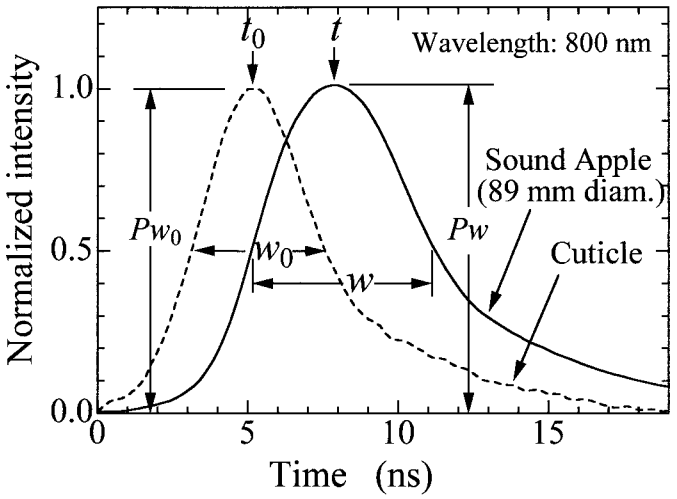

Fig. 2. Normalized time resolved profile of the transmitted output power. The equator of the apple was irradiated vertically with a pulsed laser beam of λ = 800 nm, and the transmitted output power was detected at its opposite face. The solid and broken lines represent the profiles of the apple and of its cuticle (thickness = 1.0 mm), respectively.

detection of water cores (wavelength of the laser beam and detection position of transmitted light) were investigated in detail. The authors tried to find not only wavelength-dependent characteristics, but also time-dependent characteristics of experimental data by using a simple processing method. Finally, basic data were collected to develop an in-process measurement system for practical use by the apple industry.

Material and Methods

Measuring apparatus. A schematic diagram of the measuring system used is illustrated in Fig. 1. The system consisted of an exciter laser (Surelite I-10, Continuum Electro-Optics Inc., Santa Clara, Calif.), an optical parametric oscillator (X2852, HAMAMATSU Photonics Co., Hamamatsu, Japan), a monochromator (SG-250 KOKEN KOGYO Co., Tokyo, Japan), a near infrared photoelectric multiplier (R5509-71, HAMAMATSU Photonics Co., Hamamatsu, Japan), and a digital oscilloscope (Model 9362, LeCroy Co., Chestnut Ridge, N.Y.). A Q-switched Nd: YAG laser having an output energy of 60 mJ/pulse at 335 nm, a pulse width of 5 ns, a pulse repetition frequency of 10 Hz, and a beam diameter of 6 mm was employed as the exciter laser. The wavelength of the pulsed laser (l) was tuned from 550 nm to 1100 nm by the optical parametric oscillation of a BBO (β-BaB_2O_4) crystal (Harper and Wherrett, 1975). The output power of the tuned laser beam ranged from 8 mJ/pulse (at 550 nm) to 5 mJ/pulse (at 1100 nm). However, in this power range, the spectral line width of the laser beam varied with the wavelength from 1 to 2 nm. The monochromator was used to keep the spectral line width constant at 0.1 nm.

The transmitted output power from the sample was measured by a NIR photoelectric multiplier having a spectral response ranging from 300 to 1700 nm, which was cooled to –80 °C, through an optical fiber cable having a diameter of 7 mm. An Si pin-type photodiode was placed near the optical parametric oscillator to generate a trigger signal. The optical fiber cable was directly in contact with the apple, which was enclosed in aluminum foil to keep out stray light. Furthermore, the sample, the cooling box containing the NIR photoelectric multiplier, and the optical fiber cable were also covered with black cloth. The sampling time and the number of times the transmitted output power was averaged were 100 ns and 300 times, respectively.

Outline of time resolved profile. Time resolved profile refers to the variation in intensity of the detected light beam with time. The combined effects on the time resolved profiles of the water core, the wavelength of the laser beam (l), and the detection position of transmitted light were investigated in detail. We focused on some typical parameters representing the variation of time resolved profile. The normalized time resolved profiles of a sound (non-water core) apple (89 mm in diameter) and its cuticle (thickness = 1.0 mm) are illustrated in Fig. 2. When the NIR photoelectric multiplier was used, the linearity of the input signal with respect to the photo sensitivity had to be considered. As the intensity of input pulse was very large compared to that of the transmitted output power from the sample, there may have been a stable relation between the two values. Therefore, the time resolved profile of the cuticle was employed as the reference of a zero value.

Variations in peak maxima, the time delay of peak maxima, and the full width at half maximum of the profile were examined under the experimental measuring conditions. The measure of attenuance (A_t) was defined as follows:

$$A_t = \log(P_{w0}/P_w) \quad [1]$$

where P_{w0} and P_w indicate the peak maxima of the reference and the object, respectively. The measure of time delay of peak maxima (Δt) was expressed as follows:

$$\Delta t = t - t_0 \quad [2]$$

where t_0 and t indicate the time at peak maxima of the reference and the object, respectively. The variation of the full width at half

Table 1. Specific parameters of 'Fuji' apples used to test for water core using TOF-NIRS. Rank of water core is explained in the materials and methods.

Classification of water-cored tissue[z]	Fruit diam (mm)	Fruit wt (g)	Soluble solids concn (%)
Rank 0	89	330	13.4
Rank 1	91	336	13.4
Rank 2	88	333	13.1
Rank 3	85	321	13.8

[z]See Fig. 3 for illustration of the various degrees of water core.

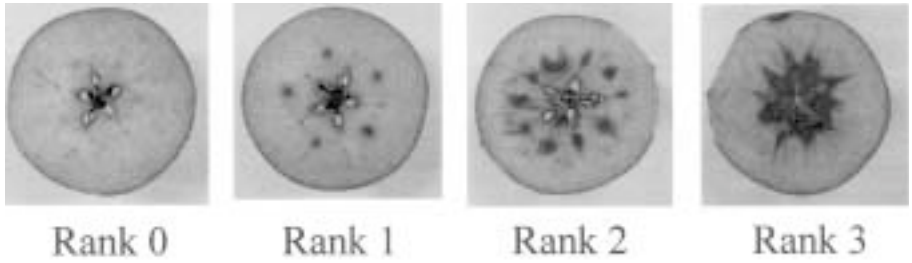

Fig. 3. Cross sections of tested apples. In visual evaluation, a scale of Rank 0 was assigned for a sound apple (nonwater core fruit) to Rank 3 for apples having extensive water core.

maximum value of the profile (Δw) was also expressed as follows:

$$\Delta w = w - w_0 \qquad [3]$$

where w_0 and w indicate the full width at half maximum value of the profile for the reference and the object, respectively.

Fruit samples. The samples used were 'Fuji' apples harvested 10 to 15 Nov. 2000 from an orchard in Nagano, Japan. Since studies were aimed to determine the probability that nondestructive measurement of water core may be accomplished using TOF-NIRS, the number of samples was limited to four per degree of water core. Soluble solids concentration was measured by a digital refractometer (IPR 201, ATAGO Co., Tokyo, Japan).

Results and Discussion

The specific parameters tested in 'Fuji' apples are listed in Table 1. Soluble solids concentration did not vary greatly in relation to the presence and extent of water core. In visual evaluation, we used a scale of Rank 0 for a sound apple to Rank 3 for apples having solid water core as illustrated in Fig. 3. In this study, the time resolved profile was measured as illustrated in Fig. 4. First, the equator of the apple was irradiated vertically with the pulsed laser, and the detection position was varied at the equator of the apple. The distance between the irradiation position and the detection position (l) was varied from 49 mm to 91 mm (Fig. 4A). Second, the transmitted output power was detected at its opposite face, while irradiation conditions were the same as for the first experiment. The sample thickness (d) was varied from 28 to 91 mm by slicing one side of the apple (Fig. 4B).

Each sample was measured five times within a given detection position and wavelength of the laser beam. During the measurement periods, no significant changes in time resolved profile were observed. The following results are therefore presented as the average signal of five measurements.

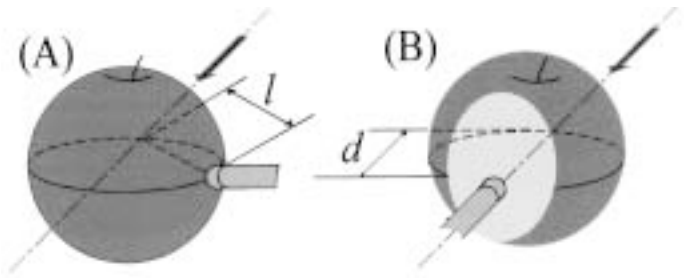

Fig. 4. Illustration of the measurement arrangement. (**A**) Distance between the irradiation position and the detection position, l, was varied from 49 to 91 mm. (**B**) Sample thickness, d, was varied from 28 to 91 mm by slicing one side of the apple.

Variation of time resolved profile in the presence and rank of water core. As a first step in this study, we investigated variation of wavelength dependency of the time resolved profile with the rank of the water core. The spectral variation of the attenuance (A_t), the time delay of peak maxima (Δt), and the variation of full width at half maximum (Δw) with the presence and rank of the water core, respectively, are presented in Fig. 5. For each sample, there were no data at ≈700 nm because of instability of the output signal.

A_t decreased gradually as the size of the water core increased independent of the wavelength. In the presence of water-cored tissue (Rank 3), we could find an output signal at ≈1000 nm which may be attributed to water absorption; however, other samples provided no data because of a strongly attenuated output signal. This means that the water-cored tissue would transmit much more energy.

A gradual decrease in Δt was also observed as the size of the water core increased; however its wavelength dependency was inversely related to A_t. When the size of the water core increases, either the intercellular spaces are filled with liquid or the cells become swollen, eliminating the air spaces and creating a translucent or water-soaked appearance. This results in less light scattering, so that the light path time through a sample decreases. In Fig. 5C, Δw shows about the same trend as Δt. Variations in these parameters are governed commonly by the wavelength dependency of light scattering and absorption characteristics, namely, scattering and absorption coefficient. We can find from the spectral response of A_t, Δt, and Δw, that the light beam at λ = 800 nm is vigorously scattered with little absorption. On the other hand, the light beam at ≈1000 nm is much attenuated or absorbed by water, so that the diffusely scattered light beams

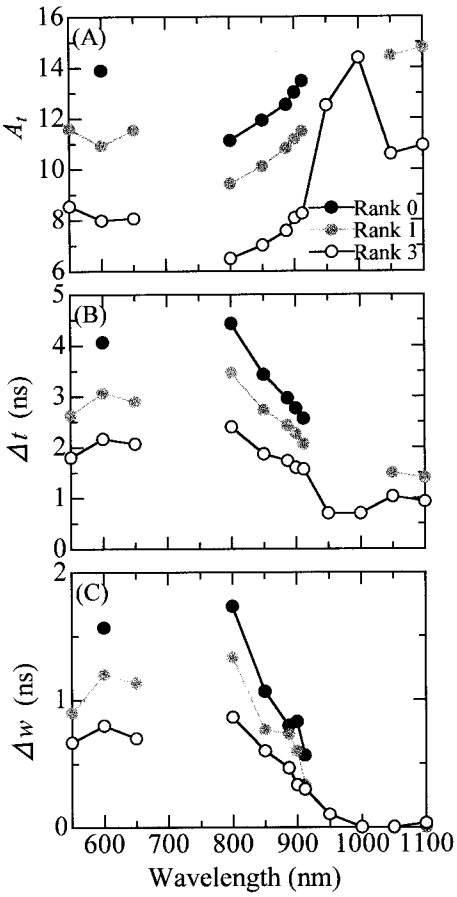

Fig. 5. Variation of wavelength dependency of time resolved profile with the rank of water core. (**A**) Attenuance (A_t), (**B**) time delay of peak maxima (Δt), and (**C**) variation of full width at half maximum (Δw). The equator of one side of a sliced apple, having a thickness of 50 mm, was irradiated vertically with the pulsed laser, and the transmitted output power was detected at the opposite face. The black, gray, and white circles indicate measured values at Rank 0, Rank 1 and Rank 3, respectively (see Fig. 3 for details) and the legend in A applies to B and C. Each symbol respects the mean of five observations.

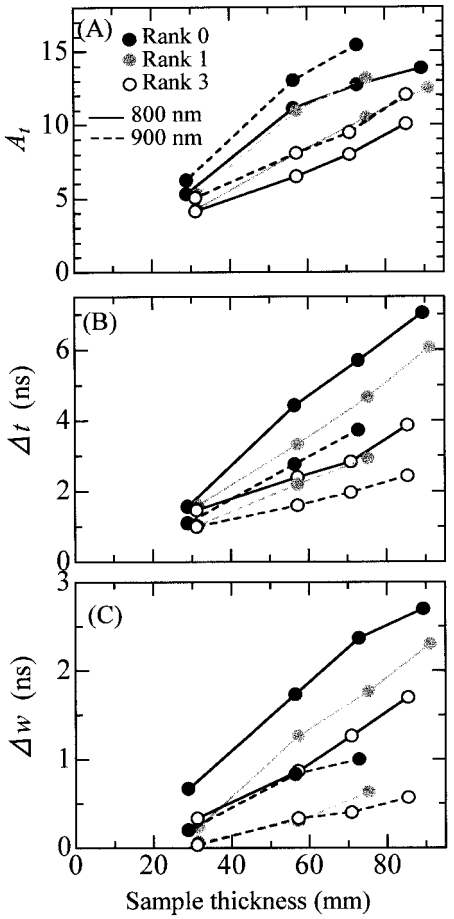

Fig. 6. Variation of time resolved profile with sample thickness. (**A**) Attenuance (A_t), (**B**) time delay of peak maxima (Δt), and (**C**) variation of full width at half maximum (Δw). The equator of the apple was irradiated vertically with the pulsed laser, and the transmitted output power was detected at its opposite face. The sample thickness d was varied from 28 to 91 mm by slicing one side of the apple (see Fig. 4B). The black, gray, and white circles indicate measured values at Rank 0, Rank 1, and Rank 3, respectively. The solid and broken lines express the results at λ = 800 nm and 900 nm, respectively. Legend in A applies to B and C. Each symbol respects the mean of five observations.

having a relatively longer optical path length hardly affect the time resolved profile.

As Birth and Olsen (1964) reported with respect to detection of water-cored apples, attention should be given to differences in the physical characteristics between sound and water-cored tissue as it affects scattering of light, and not focus on differences in composition. In the present study, the interrelation between the three parameters directly supports the aforementioned research (Birth and Olsen, 1964). Furthermore, Kays (1999) pointed out that one could find the presence of water-cored tissue by measuring the transmitted light. Such a new light transmission technique may be available to detect the defective apples as reported by Meurens and Moons (2000).

Effect of sample thickness or detection position on time resolved profile. Variation of time resolved profile with sample thickness or detection position of transmitted light was examined. Variation of A_t, Δt, and Δw with d and l, are illustrated in Figs. 6 and 7, respectively. These three parameters increased in value as d or l increased. Variation in their values for Rank 3 might have differed from others because of the presence of water-cored tissue. To interpret these results correctly, however, we considered that the characteristics of the transmitted light differed with the detection position. The output detected directly opposite to irradiation position may include the straight-through or near-straight beams (see Fig. 4B). The output at other detection positions could be defined as diffusely scattered light (see Fig. 4A). As Leonardi and Burns (1999a) reported, the difference in the optical characteristics of transmitted beams directly reflected a substantial optical path length.

Estimation of the substantial optical path length. The major substantial optical path length from the time delay of peak maxima Δt, which reflected the behavior of transmitted light was estimated. The increment of the substantial optical path length (*SOL*) from the reference was expressed as follows:

$$\mathrm{SOL} = \Delta t \times c/n_a \qquad [4]$$

where c indicates the velocity of light in vacuum space and n_a was the refractive index of apple. In this study, n_a of each sample was determined conveniently by the liquid immersion method. When the transmitted light was measured at the opposite face, the increment of a nominal optical path length (*NOL*) was defined as follows:

$$NOL = d - d_{r0} \qquad [5]$$

where d_{r0} is the thickness of an apple cuticle (1.0 mm) as reference of zero value. For measurements at the other equatorial points, the increment in *NOL* was defined as follows:

$$NOL = l - d_{r0} \qquad [6]$$

From these results, a new parameter $R_{S/N}$ was introduced as a comparable measure.

$$R_{S/N} = \frac{TOL}{NOL} \qquad [7]$$

As $R_{S/N}$ increases, the actual distance propagated by the light per unit length of the sample should increase.

Variation of $R_{S/N}$ with sample thickness at two selected wavelengths is illustrated in Fig. 8. Variation of $R_{S/N}$ with d differs somewhat according to the wavelength and the size of the water core. In the case of λ = 800 nm, the values of $R_{S/N}$ other than for Rank 3 increased as d increased. The transmitted light was not scattered sufficiently when d was small, and therefore $R_{S/N}$ remained small. However, the fact that $R_{S/N}$ for Rank 0 reached a nearly constant value suggests that the light scattering pattern in the sound cellular structure was independent of the sam-ple thickness.

For Rank 3, $R_{S/N}$ did not vary greatly with sample thickness indi-

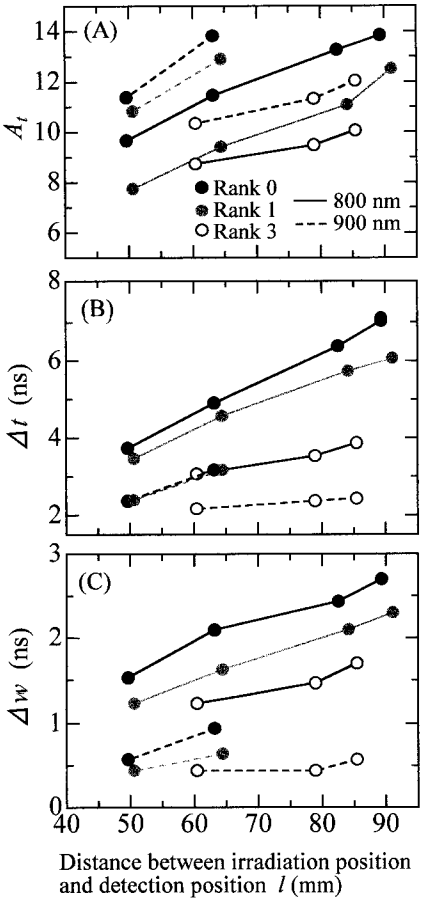

Fig. 7. Variation of time resolved profile with detection position. (**A**) attenuance (A_t), (**B**) time delay of peak maxima (Δt), and (**C**) variation of full width at half max-imum (Δw). The equator of the apple was irradiated vertically with the pulsed laser, and the detection position was varied at the equator of the apple. The distance between the irradiation position and the detection position l was varied from 49 to 91 mm (see Fig. 4A). The black, gray, and white circles indicate measured values at Rank 0, Rank 1, and Rank 3, respectively. The solid and broken lines express the results at λ = 800 and 900 nm, res-pectively. Legend in A applies to B and C. Each symbol respects the mean of five observations.

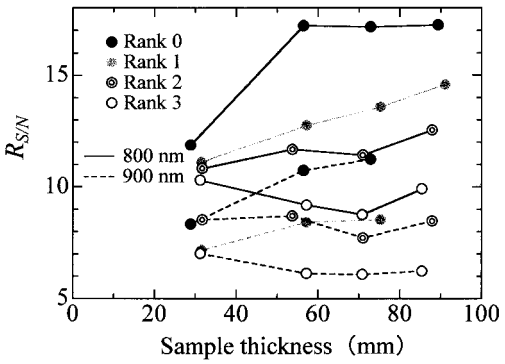

Fig. 8. Variation of the ratio of substantial optical path length to the nominal optical path length ($R_{S/N}$) with sample thickness. The equator of the apple was irradiated vertically with the pulsed laser, and the transmitted output power was detected at its opposite face. The sample thickness (d) was varied from 28 to 91 mm by slicing one side of the apple (see Fig. 4B). The solid and broken lines indicate $R_{S/N}$ values at λ = 800 and 900 nm, respectively. The black, gray, double, and white circles indicate calculated values for Ranks 0, 1, 2, and 3, respectively. Each symbol respects the mean of five observations.

cating that it may be easy for the laser beam to travel straight because of the presence of a water core. These variations with the presence and size of water cores are reduced at λ = 900 nm where the light beam is absorbed much more than for λ = 800 nm. We may estimate the substantial optical path lengths at λ = 800 nm became approximately nine to 17 times as long as sample thickness. On the other hand, the substantial optical path lengths at λ = 900 nm was six to 11 times as long as sample thickness. The authors have examined $R_{S/N}$ for wood and found that it also varied characteristically with the wavelength of the laser beam (Tsuchikawa et al., 2000a).

Variation of $R_{S/N}$ with l, for which the detection position was varied on the fruit equator is presented in Fig. 9. The value of $R_{S/N}$ for each sample at λ = 800 nm was almost constant regardless of the detection position, whereas $R_{S/N}$ decreased as the size of the water-cored tissue increased. The laser beam of λ = 800 nm was scattered vigorously, so that the transmitted light around the equator acts in a fashion similar to isotropic scattering. On the contrary, the value of $R_{S/N}$ at λ = 900 nm may have decreased slightly as l increased, that is, the value of $R_{S/N}$ at the face directly opposite the incident position of laser beam was smaller than that at the side face. In Fig. 9, the output at l = 49 to 84 mm was comprised of the diffusely scattered light whereas that at l = 85 to 91 mm may include the straight or near-straight propagating light. As it is relatively easy for light of λ = 900 nm to travel straight, we may find a difference in the characteristics of light components according to the detection position.

Optimum optical parameter for detecting water cores.

Fig. 9. Variation of the ratio of substantial optical path length to the nominal optical path length ($R_{S/N}$) with detection position. The equator of the apple was irradiated vertically with the pulsed laser, and the detection position was varied at the equator of the apple. The distance between the irradiation position and the detection position (l) was varied from 49 to 91 mm (see Fig. 4A). The solid and broken lines indicate the $R_{S/N}$ values at l = 800 and 900 nm, respectively. The black, gray, double, and white circles indicate calculated values for Ranks 0, 1, 2, and 3, respectively. Each symbol respects the mean of five observations.

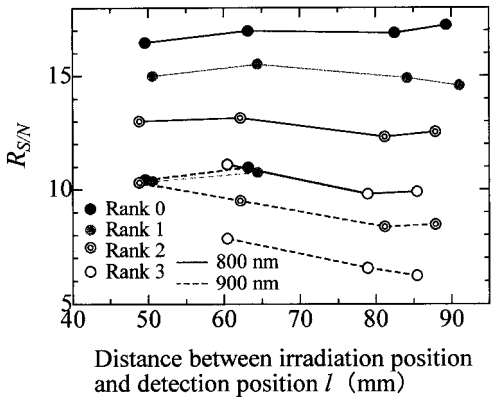

The time resolved profile varied characteristically with the presence and size of the water core, the wavelength of the incident laser beam, and the detection position. Taking into account these results, the optimum optical parameter for detecting water cores was examined. As shown in Fig. 5, the incident beam of λ = 800 nm may be strongly affected by the presence of a water core. Then, each optical parameter (A_t, Δt, and Δw) at λ = 800 nm measured on the equator was standardized by dividing by l to cancel the effect of detection position.

The relationship between the water core rank and A_t, Δt, or Δw standardized by l is presented in Fig. 10. The fluctuation of $\Delta t/l$ with detection position was very small and it differed clearly with the presence of a water core. Classification of water-cored condition is mostly visual and sensory, however, we can find it reliably by measuring Δt. The fluctuation of A_t/l with detection position is relatively large and the variation of $\Delta w/l$ with the rank of water core is small. Therefore, these parameters are not suitable for detection of water cores. These trends were generally the same at other wavelengths.

Conclusions

In this study a newly constructed optical measurement system, whose main components were a parametric tunable laser and a near infrared photoelectric multiplier, was applied to detection of water core in apples using TOF-NIRS. The combined effects on the time resolved profiles of water cores, the wavelength of the laser beam, and the detection position of transmitted light were investigated in detail. Variation in the attenuance of peak maxima (A_t), the time delay of peak maxima (Δt), and the variation of full width at half maximum (Δw) decreased gradually as the size of the water core area increased. The water-cored tissue would be expected to transmit much more energy because of the filling of the intercellular spaces with liquid. This results in less light scattering, so that the light path time through a sample decreased. The output detected at the opposite face may include straight or near-straight transmitted beams, whereas that at other equatorial detection positions may be defined as the diffusely scattered beams. To correctly interpret the behavior of the transmitted laser beam, we must take into account these results.

The substantial optical path length was estimated from Δt, and the ratio of the substantial path length to the nominal optical path

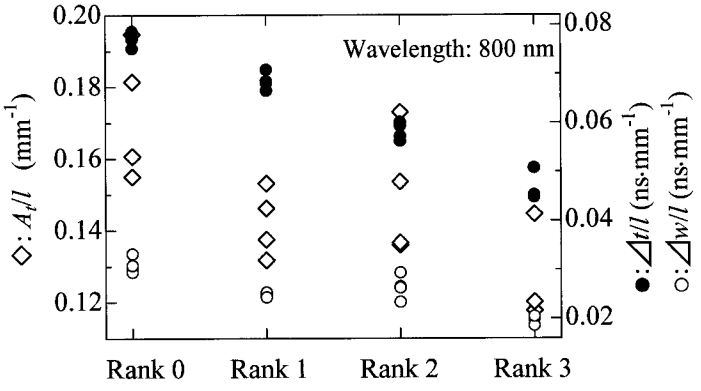

Fig. 10. Relationship between the rank of water core and A_t, Δt, or Δw standardized by dividing by l. (◇ = A_t/l, ● = $\Delta t/l$, and ○ = $\Delta w/l$, respectively). The equator of the apple was irradiated vertically with the pulsed laser, and the detection position was varied at the equator of the apple. The distance between the irradiation position and the detection position (l) was varied from 49 mm to 91 mm (see Fig. 4A). Each symbol respects the mean of five observations.

length $R_{S/N}$ was calculated. Variation of $R_{S/N}$ with sample thickness or detection position differed somewhat according to the presence and size of the water core and the wavelength of the laser beam. We estimate that the value of $R_{S/N}$ on the equator at $\lambda = 800$ nm was ≈10 to 17 while that for $\lambda = 900$ nm varied from six to 11. Fluctuations of Δt standardized by the distance between the irradiation position and the detection position is very small and it differs clearly with the presence and size of a water core. Thus, one can reliably detect the water-cored condition by Δt, although present classification of water core is generally visual and sensory.

Literature Cited

Birth, G.S. and K.L. Olsen. 1964. Nondestructive detection of water core in 'Delicious' apples. Proc. Amer. Soc. Hort. Sci. 85:74–85.

Burns, D.A. and E.W. Ciurczak. 1992. Handbook of near-infrared analysis. Marcel Dekker, New York.

Cho, R., M. Sohn, and Y. Kwon. 1998. New observation of nondestructive evaluation for sweetness in apple fruit using near infrared spectroscopy. J. Near Infrared Spectroscopy 6:A75–78.

Harper, P.G. and B.S. Wherrett. 1977. Nonlinear optics. Academic Press, New York.

Hwang, I. and S. Noh. 2000. Preliminary study for the development of an algorithm for on-line analysis of the sugar content of intact fruits using near infrared spectroscopy. Proc. 9th Intl. Near Infrared Spectroscopy Conf. p. 379–384.

Kays, S.J. 1999. Non-destructive quality evaluation of intact, high-moisture products. NIR News 10:12–15.

Leonardi, L. and D.H. Burns. 1999a. Quantitative measurements in scattering media: Photon time-of-flight analysis with analytical descriptions. Appl. Spectroscopy 53:628–636.

Leonardi, L. and D.H. Burns. 1999b. Quantitative mutiwavelength constituent measurements using single-wavelength photon time-of-flight correction. Appl. Spectroscopy 53:637–646.

Meurens, M. and E. Moons. 2000. High performance of a low-cost visible near infrared spectrophotometer. Proc. 9th Intl. Near Infrared Spectroscopy Conf. p. 125–126.

Osborne, B.G., T. Fearn, and P.H. Hindle. 1993. Practical NIR spectroscopy with applications in food and beverage analysis. Longman Scientific and Technol., Harlow, United Kingdom.

Profio, A.E. 1989. Light transport in tissue. Appl. Optics 53:2216–2221.

Sevick, E.M., B. Chance, J. Leigh, S. Nioka, and M. Maris. 1991. Quantitation of time- and frequency-resolved optical spectra for the determination of tissue oxygenation. Anal. Biochem. 195:330–351.

Tsuchikawa, S., K. Hayashi, and S. Tsutsumi. 1996. Nondestructive measurement of the subsurface structure of biological material having cellular structure by using near-infrared spectroscopy. Appl. Spectroscopy 50:1117–1124.

Tsuchikawa, S., C. Nishimura, and S. Tsutsumi. 2000a. Time-resolved near infrared spectroscopy for wood as a discontinuous body with anisotropic cellular structure. Proc. 9th Intl. Near Infrared Spectroscopy Conf. p. 95–100.

Tsuchikawa, S., T. Takahashi, and S. Tsutsumi. 2000b. Nondestructive measurement of wood properties by using near-infrared laser radiation. Forest Products J. 50:81–86.

Tsuchikawa, S. and S. Tsutsumi. 1999a. Directional characteristics model and light-path model for biological material having cellular structure. Appl. Spectroscopy 53:233–240.

Tsuchikawa, S. and S. Tsutsumi. 1999b. Analytical characterization of reflected and transmitted light from cellular structural material for the parallel beam of NIR incident light. Appl. Spectroscopy 53:1033–1039.